Raman study of thin films of amorphous-to-microcrystalline silicon prepared by hot-wire chemical vapor deposition

Daxing Han,[a] J. D. Lorentzen, J. Weinberg-Wolf, and L. E. McNeil
Department of Physics and Astronomy, University of North Carolina at Chapel Hill, Chapel Hill, North Carolina 27599-3255

Qi Wang
National Renewable Energy Laboratory, Golden, Colorado 80401

(Received 31 March 2003; accepted 11 June 2003)

The structure changes of thin films of amorphous (a) to microcrystalline (μc) silicon are studied by Raman scattering in terms of three deposition parameters: the silane flow rate, the hydrogen flow rate, and the total gas pressure in hot-wire chemical vapor deposition. The Raman transverse optical (TO) mode is deconvoluted into two Gaussian functions for a-Si:H and intermediate components and one Lorenzian function for the c-Si component. We found that (a) in general, the change in structure is a function of the ratio of hydrogen to silane gas flow, R, but also depends on the SiH_4 flow rate and total gas pressure; (b) there is a narrow structural transition region in which the short-range order of the a-Si:H network improves, i.e., the variation in bond angle of the a-Si network decreases from ~10° to ~8° once the c-Si grains start to grow; and (c) when the films were deposited using a high SiH_4 flow rate of 22 sccm, the narrow TO mode with low peak frequency could be related to the column-like structures. © *2003 American Institute of Physics.*
[DOI: 10.1063/1.1598298]

I. INTRODUCTION

Transition films of amorphous hydrogenated silicon (a-Si:H) to microcrystalline (μc) silicon have attracted a great deal of attention because the most stable, high-performance a-Si:H solar cells ever achieved were prepared just before the onset of microcrystallinity.[1] In addition, increasing crystalline silicon (c-Si) volume fraction and grain size and reducing defects are important issues for thin c-Si films and their application to devices.[2,3] Generally, the μc-Si:H structure contains an a-Si:H matrix, c-Si grains, grain boundaries (GBs), and microvoids.[4,5] Such materials exhibit a variety of microstructures and properties that depend on the preparation conditions. Compared to other deposition techniques, such as high-H dilution of plasma-enhanced chemical vapor deposition (PECVD) and very-high-frequency (VHF) PECVD,[6–8] the advantage of using the hot-wire (HW) CVD technique is its high deposition rate.[4]

Raman spectroscopy is a sensitive tool that provides valuable structural information about a-Si-based materials.[9] In a-Si, all phonon modes of the transverse acoustic (TA), longitudinal acoustic (LA), longitudinal optical (LO), and transverse optical (TO) modes are Raman active. Thus, Raman spectra of a-Si at room temperature yield a reasonable spectral comparison with phonon density of states that are modified substantially by small changes in short-range order (SRO).[8–10] Theoretical calculations have shown that the full width of half maximum (FWHM), Γ, the peak frequency of the TO phonon mode (ω_{TO}), and the relative intensity of the TA mode, TA/TO, are sensitive to variations in bond angle ($\Delta\Theta$) in an a-Si network.[8–10] Beeman *et al.*[10] found a linear relationship between the width of the TO mode and the spread in mean bond angle $\Delta\Theta$ in an a-Si network that is

$$\Gamma = 15 + 6\Delta\Theta. \tag{1}$$

More recent calculations using 1000 atom configurations[11] showed a similar relation of $\Gamma = 18.4 + 6.6\Delta\Theta$ and a shift of the TO mode frequency toward higher frequency as $\Delta\Theta$ decreases following

$$\omega_{TO} = -2.5\Delta\Theta + 505.5 \tag{2}$$

for high voltage (HV)-polarized light. Those authors[11] further found that the TA/TO intensity ratio decreases linearly with a decrease of $\Delta\Theta$. For device-quality a-Si:H, the TO mode is centered at 480 cm^{-1} with FWHM≈70 cm^{-1}. According to Eq. (1), the spread in mean bond angle $\Delta\Theta$ is ⩽10°. For c-Si, on the other hand, the Raman spectrum consists of a single sharp TO mode with FWHM of 4 cm^{-1} at frequency of 520 cm^{-1}. All other modes are not Raman active because of symmetry in the face-centered-cubic (fcc) lattice. However, when the c-Si grain size is as small as a few nm, momentum conservation will be relaxed and Raman active modes will not be limited to the center of the Brillouin zone. Thus, the frequency could shift from 520 to ≈512 cm^{-1} with a decrease in grain size from ⩾10 to ≈3 nm.[12–14] Below 3 nm, a crystalline-to-amorphous transition occurs.[14] In addition to a-Si and c-Si phonon modes, the Raman TO mode from μc-Si films contains a third intermediate peak centered around 500±10 cm^{-1}, which could be attributed to contributions by grain boundaries[4,12] or other structures.[6] With hydrogen dilution, Tsu *et al.*[6] found chainlike objects in PECVD films using high-resolution transmission electronic

[a]Electronic mail: daxing@physics.unc.edu

 © 2003 American Institute of Physics

microscopy (TEM), which they claimed is evidence of intermediate ordering in H-diluted films. They found that the *a*-Si TO band was centered at 490 cm^{-1} (37 ± 3 cm^{-1} full width) instead of at 480 cm^{-1}.

To determine the *c*-Si volume fraction from the Raman TO mode, one must take into account the differences between *a*-Si and *c*-Si with respect to scattering cross sections and optical absorption coefficients. Bustarret *et al.*[15] found that the ratio of the cross section for the amorphous-to-crystalline phase for grain size >3 nm at excitation wavelength 514.5 nm can be written as

$$y(L)=0.1+\exp[-(L/250)]. \tag{3}$$

It is expected that $y(L)$ will be 2.4 times smaller at 632.8 nm excitation. Based on the above argument, we deduced the crystalline volume fraction, X_c, from Raman TO mode using

$$X_c=(I_c+I_{GB})/[I_c+I_{GB}+y(L)I_a], \tag{4}$$

where I_c+I_{GB} and I_a are integrated intensities of the *c*-Si, intermediate and *a*-Si peaks, respectively; $y(L)$ decreases from 1 to 0.4 when grain size L grows from 3 to 30 nm. We found that when using 514.5 nm laser front excitation, X_c can be deduced in such a way as to be consistent with the results from x-ray diffraction (XRD) for HW-CVD transition films.[4,16] In previous work,[4,16] we reported Raman, XDR, Fourier transform infrared (FTIR), photoluminescence (PL), and optical absorption results for HW-CVD films with either a varying hydrogen-to-silane ratio, *R*, with fixed silane flow rate or a varying substrate temperature, T_s, at fixed $R=3$. We observed a blueshift of the *a*-Si:H PL peak frequency, which was due to narrowing of the band tail states by hydrogen dilution and a low-energy PL band in the μc-Si films. The low-energy PL band originates from the *c*-Si GB regions, and thus, we have attributed the intermediate component of the Raman TO mode to GB regions.[4,16] Previous Raman results showed a threshold of $R\approx2$ at $T_s=240$ to -250 °C and $T_s\approx200$ °C at $R=3$ for the structural transition from *a*- to μc-Si:H. Both the threshold growth conditions of crystallinity and crystalline silicon volume fraction deduced from the Raman TO modes are consistent with the results from x-ray diffraction.[4,16] In this work, we have extended our deposition parameter range to include not only the H-dilution ratio *R*, but also the effect of silane flow rate and total gas pressure. For example, at fixed *R*, the individual SiH_4 and H_2 flow rates can be changed such that one has a higher silane flow rate than the other. The films deposited at the same *R* were not the same and depended on the actual gas flow rates. This systematic study of the correlation between material structure and deposition conditions can help us understand the growth mechanism and adjust the growth conditions of μc-Si:H films.

II. SAMPLE AND EXPERIMENT

We deposited 125 intrinsic Si films by HW CVD onto Corning 1737 25×25 mm^2 glass using a combined deposition method.[17] All of the films were grown at the same substrate temperature, $T_s=240$ °C. There were four groups with various silane flow rates of 3, 8, 16, and 22 sccm, respectively. The hydrogen flow rate for each group was varied from 0 to 216 sccm. The total gas pressure was controlled by adjusting the throttling valve position (TVP) at 45%, 50%, 60%, 70%, and 80%. The higher the percentage the lower the pressure. The total pressures of the deposition chamber as a function of the TVP and H_2 flow rate is listed in Tables I–IV for $SiH_4=3$, 8, 16, and 22 sccm, respectively. For the films with low silane flow rate of 3 sccm, the thickness was controlled in the range of 1500–2000 Å, and the growth rate was in the range of 1–3 Å/s; for the films with silane flow rates of 8 and 16 sccm, the thickness was controlled in the range of 5000–6000 Å, and the growth rate was in the range of 5–13 Å/s; for the films with a silane flow rate of 22 sccm, the thickness was controlled in the range of 0.9–1.1 μm, and the growth rate was within the range of 8–21 Å/s. Two films were made as thin as the penetration depth of the 514.5 nm laser, 60–70 nm, and they were used to calibrate the Raman spectra from back excitation.

TABLE I. Total gas pressure as a function of the TVP at $SiH_4=3$ sccm.

	TVP (%)			
	45	50	60	70
H_2 (sccm)	Total gas pressure (mTorr)			
0	12	7	4	3
3.6	13	9	5	4
9	20	12	7	5
12.6	25	14	8	6
30.6	47	30	14	26
54	75	47	21	35
108	139	88	37	45
216	267	172	77	56

Raman spectra were measured using an *XY* triple spectrograph equipped with a LN_2-cooled charge coupled device (CCD) detector. The data were taken at room temperature using the 514.5 nm line of an argon-ion laser. The spectral resolution was approximately 0.5 cm^{-1} in a frequency range of 100–1000 cm^{-1}. The frequency of the Raman lines was calibrated using the TO mode of a (111) *c*-Si wafer at 520 cm^{-1}. The power of the laser was kept below the level that would thermally induce crystallization. The penetration depth of the 514.5 nm light is ~60 nm for *a*-Si:H and is larger for μc-Si:H. Since the Raman spectra reveal the

TABLE II. Total gas pressure as a function of the TVP at $SiH_4=8$ sccm.

	TVP (%)			
	45	50	60	70
H_2 (sccm)	Total gas pressure (mTorr)			
0	24	14	10	4
9	36	20	14	6
16.2	45	25	18	8
23.4	54	30	21	10
30.6	64	36	25	11
54	95	53	36	17
75.6	120	69	46	21
151.2	210	121	84	40

TABLE III. Total gas pressure as a function of the TVP at SiH_4 = 16 sccm.

	TVP (%)			
	50	60	70	80
H_2 (sccm)	Total gas pressure (mTorr)			
0	25	12	7	6
9	30	15	9	7
16.2	35	18	11	9
30.6	44	22	13	11
45	49	27	15	13
61.2	59	31	18	16
75.6	66	36	21	18
153	109	60	38	33

structure of the thin layer, measurements were also done from back excitation for most samples. To depress the scattering light from the substrate, the light spot was focused onto the film using a microscope. The Raman TO mode for all films was deconvoluted into two Gaussian functions and one narrow Lorenzian function to represent the three components of *a*-Si, intermediate, and *c*-Si peaks. The *c*-Si grain size ranged from 7 to 30 nm, and was obtained from XRD;[4] the crystalline volume fraction, X_c, was deduced using Eqs. (3) and (4) with $0.4<y(L)<0.85$.

III. RESULTS AND DISCUSSION

In general, the change in structure is a function of the ratio of hydrogen-to-silane flow, R.[4,16] Figures 1(a)–1(p) show the crystalline silicon volume fraction, X_c, as a function of R for four groups of films at SiH_4 flow rates of 3, 8, 16, and 22 sccm with the total gas pressure varied according to throttling valve position, 45%, 50%, 60%, 70%, and 80%. The solid and dotted lines indicate X_c obtained from the top and bottom layers, respectively. X_c is found from 0% to >90% (including X_{GB} from 0%–~30%) in the top layers. In agreement with previous work,[4,16] there is a threshold R for the structural transition from *a*- to μc-Si:H. The common features of the curves in Figs. 1(a)–1(p) are (1) narrow structure transition region ($\Delta R \sim 1$) from $X_c=0$ to $\geqslant$50%. We will analyze this transition region in detail shortly. (2) The threshold R of crystallinity increases with an increase in SiH_4 flow rate. For instance, the threshold is $R \leqslant 2$ for low SiH_4 flow rates of 3 and 8 sccm, as shown in Figs. 1(a)–1(g), but no crystallinity has yet occurred at $R=2$ for high SiH_4 flow rates of 16 and 22 sccm, as shown in Figs. 1(i)–1(p). (3) X_c changes with the total pressure in the chamber in the following way: the films easily become μc-Si at higher pressure (lower TVP) and lower silane flow rates of 3 and 8 sccm, as seen by comparing Figs. 1(a)–1(d) and 1(e)–1(h); whereas, at high silane flow rates of 16 and 22 sccm, lower pressure (higher TVP) yields higher X_c in the film, as seen by comparing Fig. 1(i) to Fig. 1(j) or Fig. 1(m) to Fig. 1(n). These surprising results suggest that there is a "growth zone" for the crystallite, and it is our intention to study many deposition parameters, not just R, to examine this further. We explain results (2) and (3) above by qualitatively using the silane-depletion model. At low flow rate and low pressure, the SiH_4 is almost depleted, but at high flow rate and high pressure, the SiH_4 is partially depleted. The higher the degree of SiH_4 depletion, the more the crystallinity in the films.

We used back excitation to study early growth of the film. At the early stage of growth, X_c is much lower than in later growth of the films, as shown by the dotted lines in Fig. 1 whereas in Fig. 1(d) for the film with $R=72$ and SiH_4 = 3 sccm, we observe roughly the same value of X_c. This is because film thickness of 70 nm is close to the penetration depth of the 514.5 nm laser. For such a thin sample, the Raman spectral line shape from back excitation was almost identical to that from front excitation. Indeed, the width of the *a*-Si TO mode was broader (80 cm^{-1}) and X_c was lower (57%) for back excitation compared to FWHM= 67 cm^{-1} and $X_c=63\%$ for front excitation due to the uniformity of both the absorption coefficient and the structure along the vertical direction. For all of the films in this study, the FWHMs of the *a*-Si network of the bottom layers are in the range of 75–83 cm^{-1}. These values are always broader than the 67–80 cm^{-1} of the top layers. This implies that the *a*-Si:H network near the glass substrate is less ordered compared to the top surface layer.

Figures 2(a) and 2(b) show the Raman spectra and their fitting functions for the films with SiH_4 flow of 3 sccm, TVP=45%, and $R=1$ and 2, respectively. The fits for the TA mode peaked at 145 cm^{-1} and the LA mode peaked at 330 cm^{-1}, which are also shown. The signal between the TO and LA modes is attributed to the LO mode. In comparing Figs. 2(a) and 2(b), one can see that the intensity ratio of TA/TO decreased as the film became more crystallized. This agrees qualitatively with theoretical calculations.[11] More important, we obtain structural information from the TO mode according to Eqs. (1) and (2). Figures 2(c) and 2(d) show enlarged TO mode fits between 450 and 550 cm^{-1} for the same samples as those in Figs. 2(a) and 2(b). The bandwidth of the TO mode, the FWHM, and their peak frequency, ω_{TO}, as a function of the H-dilution ratio are plotted in Figs. 3(a) and 3(b) for all the films in this study. Generally, the FWHM decreases and the ω_{TO} increases in the narrow structural transition region and then reaches saturation. Notice that the films with high SiH_4 flow rate of 22 sccm (the big crosses) show the narrowest FWHM and lowest ω_{TO}. This is perhaps

TABLE IV. Total gas pressure as a function of the TVP at SiH_4 = 22 sccm.

	TVP (%)			
	50	60	70	80
H_2 (sccm)	Total gas pressure (mTorr)			
0	33	16	10	8
21.6	45	22	14	11
30.6	50	24	16	12
41.4	57	28	18	14
52.2	61	28	20	17
57.6	65	32	21	18
82.8	79	39	26	22
198	148	76	54	48

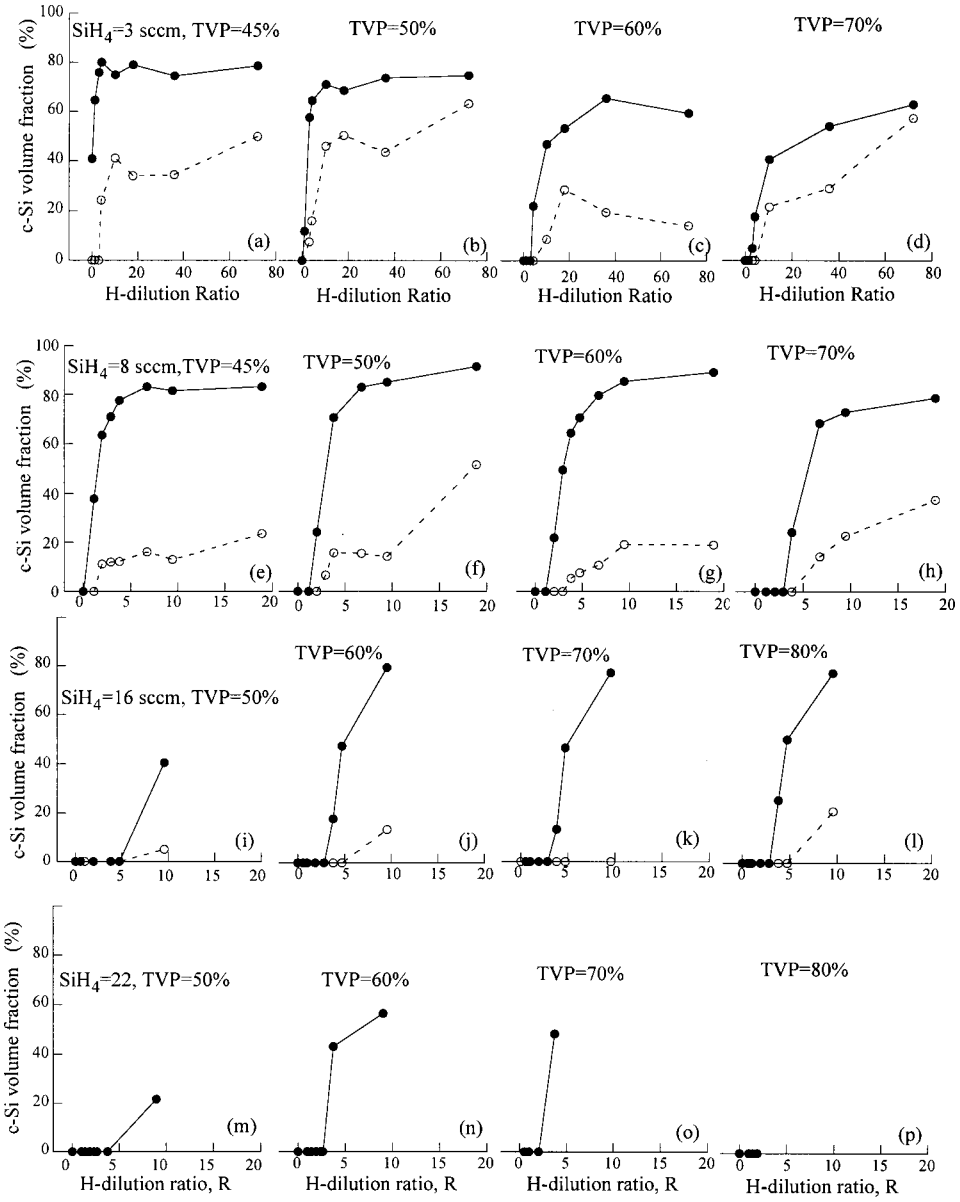

FIG. 1. Crystalline volume fraction as a function of the H-dilution ratio at SiH_4 flow rates of 3, 8, 16, and 22 sccm. The solid and dotted lines indicate X_c obtained from a top or bottom layer of $\geqslant$60 nm, respectively.

related to column-like structures.[18] The changes can be seen more clearly for the low growth rate films with SiH_4 flow rate of 3 sccm, which are represented by solid dots in both Figs. 3(a) and 3(b).

The improvement of SRO of the *a*-Si:H network in the *a*-to-μc-Si transition region is clearly seen in the changes of both the FWHM and ω_{TO}. In Fig. 3(a), the FWHM decreases from 80 to 67 cm^{-1} when $0 \leqslant R \leqslant 3$, and then remains at 67 cm^{-1} when $R > 3$. This indicates that the spread in mean bond angle $\Delta\Theta$ decreased from 10.8° to 8.6° according to Eq. (1). The corresponding shift in frequency ω_{TO} for the same films in Fig. 3(b) is from 475 to 480 cm^{-1}, which indicates that $\Delta\Theta$ decreased from 12.2° to 10.2° according to Eq. (2). The absolute values of $\Delta\Theta$ are relatively large from calculation,[11] but the 2° improvement of the bond angle spread is consistent with the results from the decrease of the bandwidth.[10] The improvement of SRO of the *a*-Si network by increasing H dilution is consistent with the observations of narrowing of the valence band tail in our previous work.[4,19] For most of the high-SiH_4 flow rate films, indicated by open circles and big crosses in Fig. 3, the FWHM $= 67$ cm^{-1} and does not change with *R*, but the ω_{TO} spreads from 475 to 480 cm^{-1} at $0 < R < 3$ whereas the FWHM is as narrow as 58.5 cm^{-1} and the peak frequency as low as 472 cm^{-1} for the films deposited with the highest growth rate of $\sim$20 Å/s (represented by the big crosses). The frequencies of the *c*-Si and GB peaks for those films are also low (see Figs. 4 and 5). Since column-type growth occurs in such conditions,[18] it implies that both the ω_{TO} and the FWHM are sensitive to the column structures. To our knowledge, there are no calculations of how the phonon density of states changes with such structures.

For the *c*-Si component, we generally found that the width of the *c*-Si TO mode for the μc-Si:H films is broader than that for the *c*-Si wafer, i.e., 8–10 cm^{-1} compared to 4 cm^{-1}. There were two exceptions for films with $SiH_4 = 3$ sccm with TPV = 70% and $R = 1.2$ and 3. The reason is unclear why the FWHM was as narrow as 4 cm^{-1} for those two films. However, the peak frequency of the *c*-Si TO

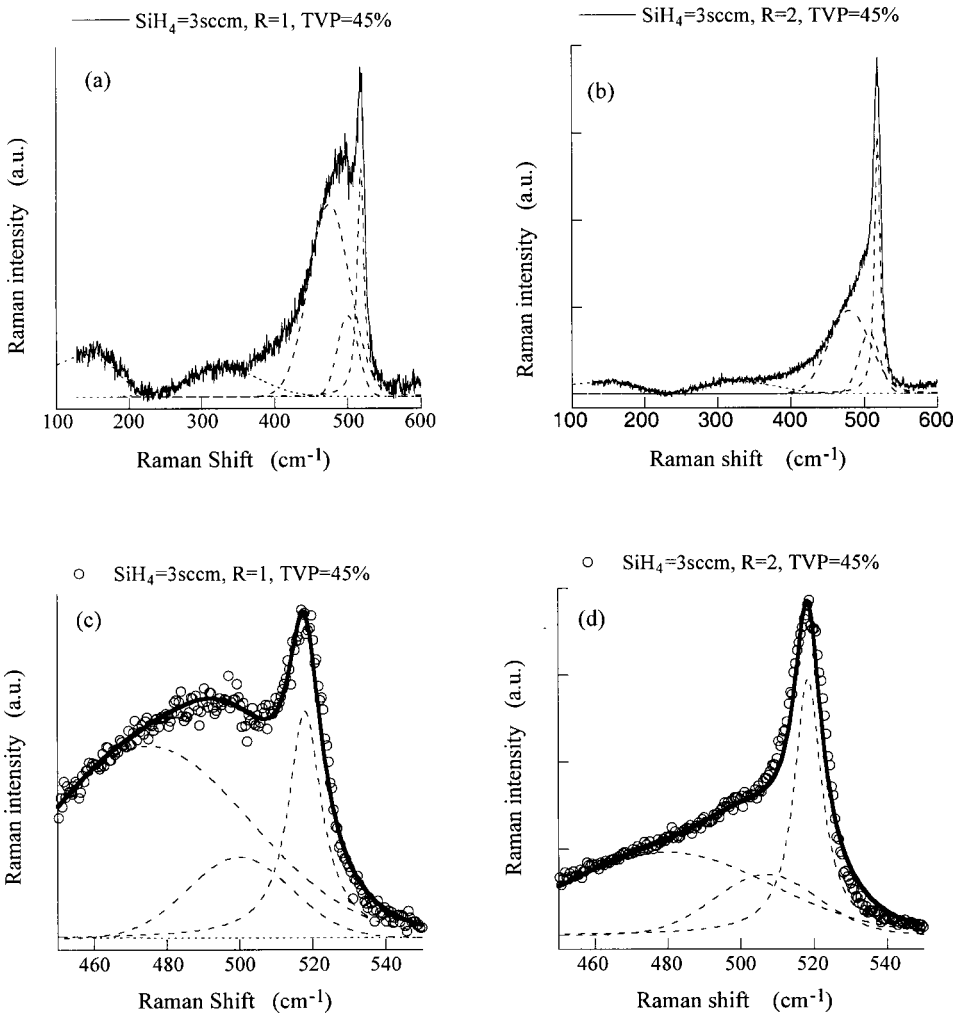

FIG. 2. Raman shift and fitting functions of films with SiH_4 flow of 3 sccm, TVP=45%, and (a) $R=1$ with fitting functions of $c1=330\times\exp\{-[(c0-475)/40]\wedge 2\}$, $c2=118\ 00/[(c0-518)\wedge 2+5.5\wedge 2]$, $c3=140\exp\{-[(c0-500)/20]\wedge 2\}$, $c4=80\exp\{-[(c0\text{-}145)/50]\wedge 2)$, and $c5=50\exp\{-[(c0-330)/70]\wedge 2\}$; (b) $R=2$ with fitting functions of $c1=480\exp\{-[(c0-480)/40]\wedge 2\}$, $c2=300\ 00/[(c0-518.5)\wedge 2+4.5\wedge 2]$, $c3=350\exp\{-[(c0-507)/20]\wedge 2\}$, $c4=75\exp\{-[(c0-145)/50]\wedge 2\}$, and $c5=70\exp\{-[(c0-330)/70]\wedge 2\}$; and the enlarged TO mode between 450 and 550 cm^{-1} with their fitting functions of $c1+c2+c3$ in (c) and (d).

mode, $\omega_{c\text{-Si}}$, changes when R increases. For the films with SiH_4 flow rates of 3 and 8 sccm, we found a blueshift from 516 to 520 cm^{-1} in the transition region, as shown in Fig. 4. This indicates that the crystallite size has increased from ~7 to ≥10 nm.[12–14] For the films with high SiH_4 flow rate of 22 sccm, the big crosses indicate that the $\omega_{c\text{-Si}}$ blueshift occurs from 513 to 518 cm^{-1}. Again, the relatively low frequency of the *c*-Si TO mode could be due to the column-like structures.

Finally, for all the μc-Si:H films, the Raman TO mode always contains an intermediate component in addition to the *a*-Si and *c*-Si components. The intermediate component was fitted well using a Gaussian function with FWHM of 33 cm^{-1} for all the μc-Si:H films. The peak frequency of the intermediate component, ω_{GB}, as a function of R is plotted in Fig. 5. One finds that the value spreads from 500 to 510 cm^{-1}. For the low-growth rate films, there is a blueshift of ω_{GB} from 500 to 507 cm^{-1} in the transition region that then spreads between 505 and 507 cm^{-1} when $R>3$. Regardless of whether or not the intermediate component originates from the grain boundaries, small size (<3 nm) crystallites,[4,12] or median-range ordered objects,[5] the blueshift of ω_{GB} can be attributed to growth of the *c*-Si grain size. One may argue that Raman modes reflect SRO and that the phonon density of states is sensitive to local bond angles.[9–11] However, the scattering intensity is related to the coupling-parameter-weighted phonon density of states. Small differences between peak positions could be attributed to changes in median- or long-range interactions that are consequences of the coupling parameter. We could not clarify the origin of this intermediate component in this work. Whatever the origin is, one commonly takes the third component into account as part of the *c*-Si volume fraction, as seen in Eq. (4).

As shown above, the peak frequencies of all the three components of the TO modes show a blueshift with an increase of H dilution in the structural transition region. The compressive stress could be higher in films with higher hydrogen dilution ratios (the film easily peels off the substrate), and the blueshift of the phonon bands could be partly related to an increase of film stress.

IV. SUMMARY

Raman scattering studies were carried out for the transition of films from amorphous-to-microcrystalline silicon prepared by HW CVD with varying silane and hydrogen flow rates and T-valve positions. The measurements were done for both front and back excitation. The TO mode was deconvoluted into a broad Gaussian function for *a*-Si:H and into a narrow Lorenzian function for *c*-Si; the Gaussian function

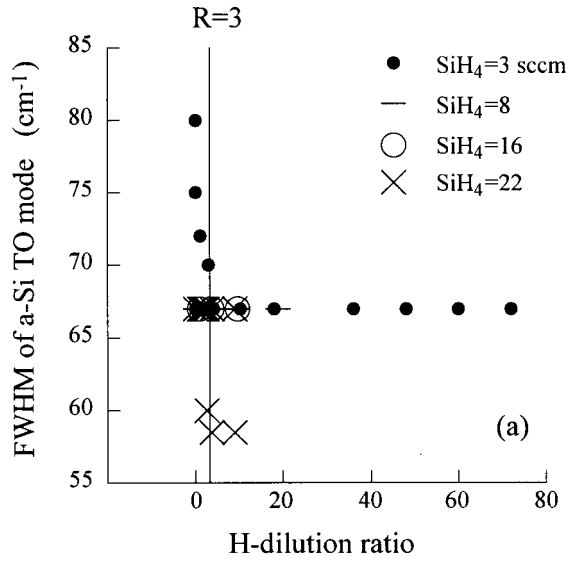

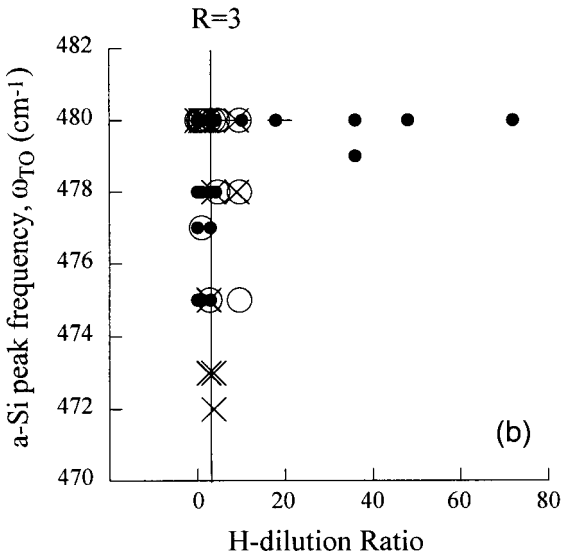

FIG. 3. (a) Bandwidth and (b) peak frequency of *a*-Si TO mode as function of the hydrogen dilution ratio. The closed dots, dashes, open circles, and crosses represent films with SiH_4 flow rates of 3, 8, 16, and 22 sccm, respectively. There are two regimes separated at $R \approx 3$: the fast changing regime when $R < 3$ and the saturated regime when $R > 3$.

peaked at between 500 and 510 cm^{-1} with FWHM of 33 cm^{-1} for the intermediate component. We believe that the origin of the intermediate component is the grain boundaries and the small size (<3 nm) of the crystallites,[4,12] and attribute it into the total *c*-Si volume fraction. The *c*-Si volume fraction depends not only on the H-dilution ratio, $R = H_2/SiH_4$, and the film thickness, but also on the SiH_4 flow rate and total gas pressure, which can be explained using the silane-depletion model. Detailed calculation of gas depletion will be reported in future work.

The most interesting finding is a narrow structural transition region of $\Delta R \sim 1$, in which short-range order of the *a*-Si:H network is improved: the width of the TO mode decreased from 80 to 67 cm^{-1} and the peak frequency, ω_{TO}, blueshifted from 475 to 480 cm^{-1}. These indicate that the bond angle variation, $\Delta\Theta$, of the *a*-Si network decreases from ~10° to ~8° when the crystallites start to grow. Furthermore, the crystallite grain size increases from ~7 to ⩾10 nm in the transition region, as evidenced by a blueshift of *c*-Si mode, $\omega_{c\text{-Si}}$, from 516 to 520 cm^{-1}.[12–14] When *R* continuously increases beyond the transition region, the SRO of the *a*-Si:H network, the *c*-Si volume fraction, and the *c*-Si peak frequency become somewhat saturated. However, the structure would be continuously modified at a higher hydrogen dilution ratio. Other techniques such as TEM will assist in clarifying further structural changes.

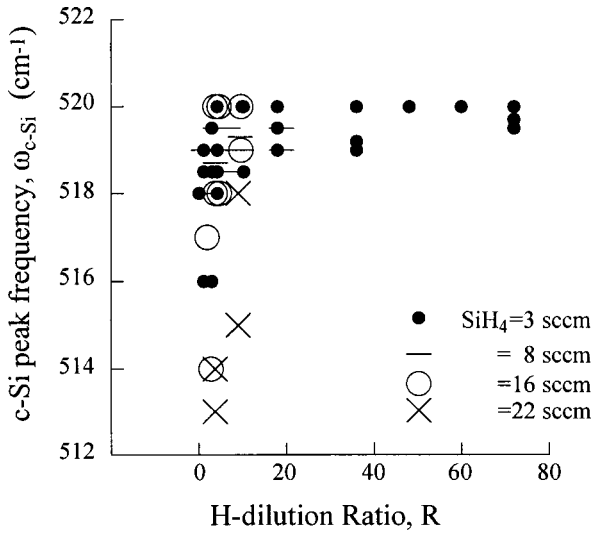

FIG. 4. Peak frequency of *c*-Si as a function of *R*.

Finally, when the films were deposited at a high growth rate ~20 Å/s using a high SiH_4 flow rate, the FWHM of the TO mode of the *a*-Si network can be as narrow as 58.5 cm^{-1} and the peak frequency as low as 472 cm^{-1}. Column-type growth occurs in such conditions,[18] which implies that both

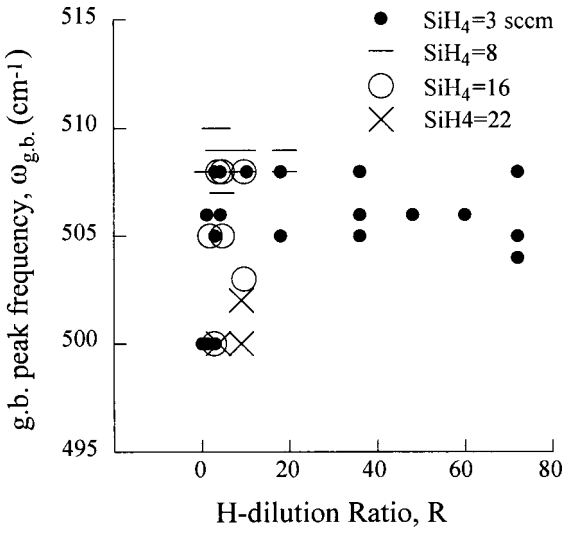

FIG. 5. Intermediate component peak frequency of TO mode as a function of *R*.

the ω_{TO} and the FWHM are sensitive to the column structures. Calculations are needed to find out how the phonon density of states changes with these structures.

ACKNOWLEDGMENT

This work is supported by National Renewable Energy Laboratory Subcontract No. ADJ-1-30630-09 at the University of North Carolina and by the U.S. Department of Energy (DOE) under Contract No. DE-AC36-99GO10337.

[1] S. Guha, J. Yang, D. L. Williamson, Y. Lubianiker, J. D. Cohen, and A. H. Mahan, Appl. Phys. Lett. **74**, 1860 (1999).
[2] J. K. Kim, J. Y. Lee, and K. S. Nam, J. Appl. Phys. **77**, 95 (1995).
[3] J. Meier *et al.*, Mater. Res. Soc. Symp. Proc. **420**, 3 (1996).
[4] G. Yue, J. D. Lorentzen, J. Lin, Q. Wang, and D. Han, Appl. Phys. Lett. **75**, 492 (1999).
[5] G. Yue, D. Han, D. L. Williamson, J. Yang, K. Lord, and S. Guha, Appl. Phys. Lett. **77**, 3185 (2000).
[6] D. V. Tsu, B. S. Chao, S. R. Ovshinsky, S. J. Jones, J. Yang, and S. Guha, Phys. Rev. B **63**, 125338 (2001).
[7] M. Luysberg, P. Hapke, R. Carius, and F. Finger, Philos. Mag. A **75**, 31 (1997).
[8] L. Houben, M. Luysberg, P. Hapke, R. Carius, F. Finger, and H. Wagner, Philos. Mag. A **77**, 1447 (1998).
[9] J. S. Lannin in *Semiconductors and Semimetals*, edited by J. L. Pankove (Academic, London, 1984), Vol. 21, Part B, Chap. 6.
[10] D. Beeman, R. Tsu, and M. F. Thorpe, Phys. Rev. B **32**, 874 (1985).
[11] R. L. C. Vink, G. T. Barkema, and W. F. van der Weg, Phys. Rev. B **63**, 115210 (2001).
[12] S. Veprek, F. A. Sarott, and Z. Iqbal, Phys. Rev. B **36**, 3344 (1987).
[13] Y. He, C. Yin, G. Cheng, L. Wang, X. Liu, and G. Y. Hu, J. Appl. Phys. **75**, 797 (1994).
[14] S. Veprek, Z. Iqbal, and F. A. Sarott, Philos. Mag. B **45**, 137 (1982).
[15] E. Bustarret, M. A. Hachicha, and M. Brunel, Appl. Phys. Lett. **52**, 1675 (1988).
[16] D. Han, K. Wang, J. M. Owens, L. Gedvilas, B. Nelson, H. Habuchi, and M. Tanaka, J. Appl. Phys. **93**, 3776 (2003).
[17] Q. Wang, G. Yue, J. Lin, and D. Han, Solid State Commun. **113**, 175 (2000).
[18] A. H. Mahan, Y. Xu, D. L. Williamson, W. Beyer, J. D. Perkins, M. Vanecek, L. M. Gedvilas, and B. P. Nelson, J. Appl. Phys. **90**, 5038 (2001).
[19] D. Han, K. Wang, and L. Yang, J. Appl. Phys. **80**, 2475 (1996).